Eur Biophys J (1993) 22:259–267

European Biophysics Journal

Solvent modulation of the structural heterogeneity in FeIII myoglobin samples: a low temperature EPR investigation

Anna Rita Bizzarri [1], **Salvatore Cannistraro** [1, 2]

[1] Unita' INFM-CNR, Dipartimento di Fisica dell'Universita', I-06100 Perugia, Italy
[2] Dipartimento di Scienze Ambientali, Sezione Chimica e Fisica, Universita' della Tuscia, I-01100 Viterbo, Italy

Received: 2 April 1993 / Accepted in revised form: 18 June 1993

Abstract. High spin FeIII myoglobin samples in solutions with different solvent composition have been investigated at low temperature by Electron Paramagnetic Resonance spectroscopy. The g = 6 line of the spectrum has been analyzed in terms of a distribution of the two crystal field parameters Δ_1 and Δ_2. By means of the Angular Overlap Method, it has been shown that these distributions entail, in turn, a distribution in the iron-heme displacement along the normal to the heme-plane. The spread in this iron-heme distance, which can be connected with the binding action of the proximal histidine, has been proposed as a quantitative measurement of the structural heterogeneity (conformational substate landscape) displayed by the protein molecules. The results point out, moreover, that the solvent composition can affect the structural heterogeneity of the protein system. In particular, addition of glycerol, ethylene glycol and sucrose yields a significant reduction in the spread of the iron-heme displacement, while the presence of ammonium sulfate induces a change in the average position of the iron in the heme-plane. The role played by the solvent in the structure and dynamics of the protein, in connection also with the conformational substate distribution, is discussed.

Key words: Myoglobin – Conformational substates – Electron paramagnetic resonance

Introduction

Proteins are dynamic structures with a time scale covering a very wide range. At temperatures below the glass temperature T_g, a protein molecule displays a solid-like behaviour characterized by harmonic oscillations for the atomic positions. On the other hand, above T_g, anharmonic motions are excited, as observed by scattering techniques (Doster et al. 1989; Parak et al. 1982); such behaviour is also related to the thermally activated transitions among slightly different macromolecular structures that are called conformational substates (CS) and whose existence has been confirmed by many experimental investigations (Frauenfelder et al. 1988; Goldanski and Krupyanskii 1989; Parak et al. 1987; Doster et al. 1989). By lowering the temperature, fluctuations among CS can be blocked and, below T_g, the protein system becomes trapped in local minima giving rise to a static distribution of substates (Elber and Karplus 1987). These presence of a CS distribution is able to affect the biological function of the protein, since the rate of the kinetic processes depends on the particular substate assumed by the macromolecule (Ansari et al. 1985).

It is well-known that the protein structure can also be modified by changing the chemico-physical properties of the solvent, so that the protein dynamics become strongly coupled to the properties of the medium; for example, addition of some organic substances, such as glycerol, ethylene glycol and sucrose yields a damping of the protein motion and then a change in the kinetic response of the macromolecule (Beece et al. 1980; Gavish and Werber 1979); such behaviour is probably related to a reorganization of the H-bond network of the solvent (Gekko and Timasheff 1981; Doster et al. 1986). In addition, the glass-temperature T_g of the protein system, below which transitions among CS are blocked, is dependent on the composition of the solvent medium (Iben et al. 1989). On the other hand, the static CS distribution, characterizing the low temperature myoglobin (Mb) samples, has also been found to be correlated with the properties of the solvent (Di Iorio et al. 1991), whose dynamics might be ultimately responsible for the structural arrest of the protein molecules in several different CS (Bizzarri and Cannistraro 1991). Moreover, it has been hypothesized that the hydration water could play a crucial role in determining the dynamics of the protein and the transitions among CS (Doster et al. 1986; Singh et al. 1981; Marzola and Cannistraro 1992). From a spectroscopic point of view, the presence of a CS distribution may result in a broadening of the detected signal. In particular, a signifi-

Correspondence to: S. Cannistraro

cant mean square displacement $\langle x^2 \rangle$ of the protein atomic positions and of the metal ion position has been detected by X-ray diffraction analysis (Parak et al. 1987; Frauenfelder et al. 1979) and by Mössbauer spectroscopy (Parak et al. 1982) performed on samples of Mb crystals. Moreover, extensive broadening of the lines has been observed, on Mb samples, by optical spectroscopy in the presence of glass-making solvents, such as glycerol or ethylene glycol (Srajer et al. 1986, Ansari et al. 1987; Di Pace et al. 1992). In our previous work (Cannistraro 1990; Cannistraro and Giugliarelli 1986; Bacci and Cannistraro 1990; Bizzarri and Cannistraro 1991) we have shown that EPR spectroscopy can be used to probe the heterogeneity characterizing the protein samples at low temperature. In particular, the analysis of the EPR spectra of high and low spin FeIII Mb samples (Bizzarri and Cannistraro 1991, 1992a,b), in terms of appropriate crystal field parameter distributions, has allowed us to demonstrate a frozen disorder around the metal ion arising from the presence of an ensemble of protein molecules in different CS. Moreover, in the case of high spin Mb, the application of the Angular Overlap Method (AOM) has allowed us to propose the observed spread of the iron-heme displacement σ_a as a quantitative estimation of the CS heterogeneity (Bizzarri et al. 1993). EPR spectroscopy has the advantage, with respect to the other techniques, that samples both in the presence and in the absence of added solvents can be studied. Accordingly, we have observed that the addition of some substances to the Mb samples may reduce the spread of the iron-heme displacement σ_a, and then the sample structural heterogeneity (Bizzarri et al. 1993).

It should be taken into account that most of the experimental results available in the literature concerning the CS distribution have been obtained in the presence of some particular solvents (used to make crystals, or to make the samples transparent). Such a consideration, together with our preliminary findings pointing out an effect of some of these solvents on the CS distribution, has led us to perform a systematic EPR analysis on the effects induced on the CS distribution by the solvents most commonly used in other spectroscopic studies. Moreover, the effects induced by the addition of sucrose, a viscous cosolvent that has been widely employed in the studies of the effects of viscosity changes on protein systems (Almagor et al. 1992) have been considered. The present spectroscopic approach, being carried out both on pure Mb samples and on Mb in the presence of different added solvents, provides a unique opportunity to analyze, in a comparative way, the structural heterogeneity of Mb in solutions with different solvent composition. Such an analysis entails a more general view about the coupling between protein structural heterogeneity and the solvent properties.

Materials and experimental methods

Mb EPR samples were prepared by dissolving commercial (Sigma Chem. Co.) lyophilized horse skeletal muscle Mb in 0.2 Mb phosphate buffer. The highest concentration of Mb in the solutions was about 5 mM and the final pH was 6.8. Ferricyanide was used to oxidize the heme iron to the FeIII valence state and the solutions were dialysed several times against buffers to remove the oxidant. Samples in the mixed water-glycerol solvent were prepared by adding glycerol to Mb solutions until the required concentration was reached. Samples in the presence of ethylene glycol were prepared in 1:1 (by volume) water-ethylene glycol mixture. Samples in the presence of sucrose were prepared in 1:1 water-sucrose (1 M solution) mixtures. Samples in the presence of ammonium sulfate were prepared in 1:1 (by volume) water-ammonium sulfate (saturated solution) mixtures. All chemicals used were of analytical reagent grade.

All the EPR spectra were recorded at 77 K (liquid nitrogen) by an X-band Varian E109 spectrometer equipped with a variable temperature control which was also used to cool the samples in a controlled way. The freezing of the bulk water during the cooling process was monitored by the appearance of a deep in the resonant cavity mode of the EPR spectrometer; such a phenomenon pointing out a decrease in the dielectric loss of samples as due to the liquid-solid transition. To calculate the experimental g-values, a magnetic field calibration was performed with a Magnion Precision NMR gaussmeter Mod. G-542; the microwave frequency being measured with a Marconi 2440 counter.

Acquisition of the EPR data was carried out on an HP 86A personal computer through a home made interface connected to an IEEE 488 bus (Giugliarelli et al. 1989). To run both simulations and bestfit programs, the same microcomputer was switched to an intelligent terminal of the main frame computer (VAX 8350), through a serial interface and an HP terminal emulator.

Analysis of the EPR spectra

All the EPR spectra of the analyzed Mb samples show the typical pattern corresponding to high spin ($S=5/2$) iron ions placed in an axially symmetric crystal field and which can be described by the spin hamiltonian

$$H_s=\beta[g_{\parallel} H_z S_z+g_{\perp}(H_x S_x+H_y S_y)] \tag{1}$$

where the Zeeman interaction of a fictitious spin $S=1/2$ is taken into account and $g_{\parallel}\simeq 2$ and $g_{\perp}=g_x=g_y\simeq 6$ are the g-values at which the two EPR resonances are actually registered; β is the Bohr magneton. The shape of the $g_{\perp}=6$ line can be better described if a small rhombic distortion ($g_x\neq g_y$) is admitted. Actually if high order corrections arising from spin-orbit mixing of the excited quartet states (^4E, $^4A_2$) ions into the ground state ($^6A_1$) of Fe^{+3} are taken into account, the following expression can be derived for g_x and g_y (Scholes 1970; Fiamingo et al. 1989; Bizzarri and Cannistraro 1991),

$$g_{x,y}=3g_e\pm 12\left[\frac{\gamma}{\Delta_2}\frac{\Delta_1}{(\Delta_2-\Delta_1)}\right]-18.7\left[\frac{\gamma}{\Delta_2}\frac{\Delta_1}{(\Delta_2-\Delta_1)}\right]^2 - \frac{12}{5}\xi^2\left[\frac{1}{\Delta_1^2}+\frac{1}{\Delta_1\Delta_2}+\frac{1}{\Delta_2^2}\right] \tag{2}$$

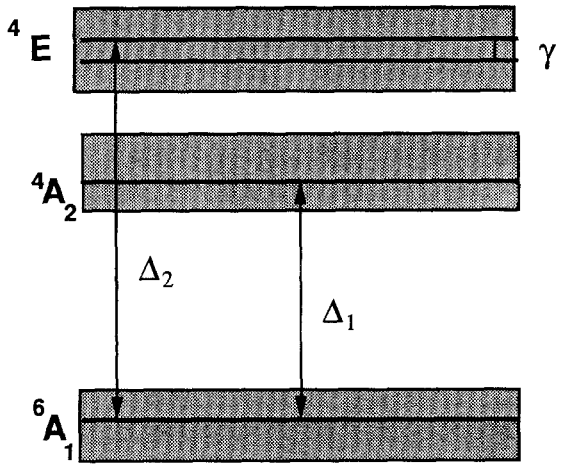

Fig. 1. Energy level diagram of the low-lying electronic states of high spin ferric heme. The shaded regions indicate the variability of the energy levels (not to scale)

where g_e is the g-factor of the free electron, ξ is the effective spin-orbit coupling constant ($\xi \sim 300\ \mathrm{cm}^{-1}$) which is reduced from the free-ion value ($\xi \sim 420\ \mathrm{cm}^{-1}$); Δ_1, Δ_2, and γ are the energy differences between the low-lying electronic states of the high spin FeIII heme (see Fig. 1). A deviation of g_x from the g_y value may result in a broadening of the $g=6$ line (as in our case) or, for a larger rhombicity, even in a splitting of this line (Peisach et al. 1971). In general, two different contributions can be assumed to be important in the Δ_1 and Δ_2 energies (Kotani 1968): one arising from the differences of the electrostatic interaction between the electronic states and another one which takes into account the energy splitting of the d-orbitals as induced by the ligand field. It can be shown that

$$\Delta_1 = [22B + 7C] + [E(\zeta) - E(\varepsilon)] \tag{3}$$

$$\Delta_2 = \tfrac{1}{2}\{[21B + 10C]\} + \tfrac{1}{2}\{[E(\eta) - E(\theta)] + \tfrac{1}{4}[E(\xi) - E(\varepsilon)]\} \tag{4}$$

where B and C are the Racah parameters and the symbols $E(\xi)$, $E(\eta)$, $E(\zeta)$, $E(\theta)$ and $E(\varepsilon)$ stand for the energies of the one electron levels d_{yz}, d_{xz}, d_{xy}, d_{z^2}, and $d_{x^2-y^2}$, respectively. Accordingly to (Abragam and Bleaney 1970), the Racah parameters are reduced from those of the free ion and take the following values: $B = 500\ \mathrm{cm}^{-1}$ and $C = 2000\ \mathrm{cm}^{-1}$. It has been shown (Bizzarri and Cannistraro 1991, 1992a), that the low temperature EPR spectra of Mb are characterized by distribution of the crystal field parameters Δ_1 and Δ_2; such a distribution, resulting in a spread of the g_x and g_y values (see Eq. (2)), taking into account the g-strain effect (Giugliarelli and Cannistraro 1985; Hagen et al. 1985; Brill et al. 1986; Yang and Gaffney 1987) that characterizes the low temperature EPR spectra of metallo-proteins. Accordingly, the Δ_1 and Δ_2 distributions can be interpreted in terms of a spread of the parameters characterizing the geometrical structure of the heme-group. To make such a connection more explicit, we have applied the AOM to the ligand-iron complex, a method particularly suitable for analyzing low-symmetry metal-complexes (Bacci 1979). In this framework, the energy change, e_λ, of a given metal orbital, as induced by the interaction with a ligand on the z-axis, is given by (Burdett 1980)

$$e_\lambda = K_\lambda S_\lambda^2 F_{\lambda\omega}^2 \tag{5}$$

where λ indicates the bonding symmetry with respect to the metal-ligand axis (σ, π being restricted our analysis to these symmetries), K_λ is a constant depending on the metal and ligand energies; S_λ depends upon the interatomic distance, the nature of atoms and the type of the orbitals. The angular term $F_{\lambda\omega}$ is a simple function of the angular polar coordinates θ, ϕ of the one atom relative to another. If the ligand is not lying on the z-axis, a rotation of the coordinate system is required. Under the assumption that the effects of different ligands are additive and that the ligand-ligand overlap can be neglected, the general ligand field matrix element can be expressed as (Schäffer 1967)

$$\langle \phi_i | V | \phi_j \rangle = \sum_{\lambda\omega} \sum_{n}^{N} e_{\lambda n} F_{\lambda\omega}(\phi_i, X_n) F_{\lambda\omega}(\phi_j, X_n) \tag{6}$$

where V is the potential induced by the ligands; the first sum on the metal orbitals is referred to a coordinate system $x'y'z'$ such that the i-ligand is on the z' axis; the second sum is extended to the N ligand X_n. $F_{\lambda\omega}(\phi_i, X_n)$ and $F_{\lambda\omega}(\phi_j, X_n)$ are the columns of the AOM rotation matrix which relates the metal orbitals in the primed and unprimed coordinate system (for the angular dependence of the Overlap Integrals see Tables in Burdett (1980)).

In order to evaluate the matrix elements in Eq. (6), the geometrical arrangement of the ligands around the metal ion and the values of the two parameters, e_σ and e_π for each ligand should be assigned. A simplified geometry for the heme group has been introduced. Specifically, in agreement with Srajer et al. (1988), it has been assumed that the iron is displaced out of the heme-plane (iron-heme plane distance $a_0 = 0.40$ Å (Takano 1977)), the four ligands of the porphyrin ring are assumed to be equivalent (the symbols e_σ^I and e_π^I have been employed to describe these parameters) and, finally, there are two axial ligands along the normal to the heme-plane (e_σ^{II}, e_π^{II}, e_σ^{III} and e_π^{III} are the symbols used to described the fifth and the sixth ligands, respectively). On the basis of data from the literature and from some empirical evaluations (Bacci 1980; Bizzarri et al. 1993) the following set for the parameters e_λ has been employed as the starting point for our analysis $e_\sigma^I \approx 10\,000\ \mathrm{cm}^{-1}$, $e_\sigma^{II} \approx 2000\ \mathrm{cm}^{-1}$ and $e_\sigma^{III} \approx 500\ \mathrm{cm}^{-1}$; moreover, $\left(\frac{e_\pi}{e_\sigma}\right)^I = 0.1$ and $\left(\frac{e_\pi}{e_\sigma}\right)^{II} = \left(\frac{e_\pi}{e_\sigma}\right)^{III} = 0.15$ have been used as fixed values (Bacci 1980; Bizzarri et al. 1993). Such an approach has allowed us to interpret the the Δ_1 and Δ_2 distributions in terms of the spread σ_a of the iron-heme displacement along the normal to the heme plane. Even if a contribution from a slight non-axial displacement of the metal ion to the Δ_1 and Δ_2 distributions cannot be ruled out, our analysis indicates that the main effect on these distributions arises from a spread in the iron position along the normal to the heme-plane.

In practice, the $g=6$ EPR line has been analyzed in terms of two independent Gaussian distribution for the crystal field parameters Δ_1 and Δ_2. According to our previous papers (Bizzarri and Cannistraro 1991, 1992a),

the simulated EPR derivative spectrum can be expressed by

$$\frac{dS(\nu_c,H)}{dH}=\frac{C\nu_c h}{\beta}\frac{1}{2\pi(\sigma_{\Delta_1}\sigma_{\Delta_2})}\int_{-\infty}^{\infty}\int_{-\infty}^{\infty}\int_{0}^{\pi/2}\int_{0}^{\pi/2}\frac{P(\theta,\phi,\Delta_1,\Delta_2)}{g(\theta,\phi,\Delta_1,\Delta_2)}\cdot\frac{df([H-H_0],\sigma_H)}{dH}\sin(\theta)\,d\theta\,d\phi\,e^{-\left[\frac{\Delta_1-\Delta_1^0}{\sigma_{\Delta_1}}\right]^2}\cdot e^{-\left[\frac{\Delta_2-\Delta_2^0}{\sigma_{\Delta_2}}\right]^2}d\Delta_1\,d\Delta_2 \quad (7)$$

where C is a constant that encompass all instrumental parameters, h is the Planck constant, ν_c is the microwave frequency. $P(\theta,\phi,\Delta_1,\Delta_2)$ is the orientation dependent transition probability which in this case can be exactly calculated (Isomoto et al. 1970). $f[(H-H_0),\sigma_H)]$ is the lineshape function, centered at the resonance field H_0, that takes into account different phenomena that are not explicitly considered. Relaxation processes are particularly relevant in this case. At the temperature of interest, the relaxation process are dominated by the spin-spin relaxation (Eisenberger and Pershan 1967) that does not significantly depend on the solvent composition of the protein solution. Consequently, all the simulations of the different Mb samples have been performed by employing the same lineshape: i.e. a Lorentzian lineshape with $\sigma_H=25$ gauss. It should be emphasized that, on the basis of an extensive lineshape analysis made by us and other authors (Bizzarri 1992; Bizzarri and Cannistraro 1991, 1992a; Hagen et al. 1985; Brill et al. 1986) the large inhomogeneous broadening (g-strain), which is superimposed on both the powder effect and the homogeneous broadening in the $g=6$ Mb line, cannot reliably be reproduced by taking into account only one value for the g-tensor, even if larger values for σ_H are used.

The computer-synthesized spectra have then been used to fit the experimental EPR spectra in order to determine the parameters Δ_1^0, Δ_2^0, σ_{Δ_1} and σ_{Δ_2} characterizing the Gaussian distributions for Δ_1 and Δ_2. The search for the bestfit parameters was done by simulated annealing approach (Kirkpatrick et al. 1983); each parameter was allowed to vary over a wide range consistent with both those estimated from the experimental spectra and those reported in the literature (Fiamingo et al. 1989).

Once the parameters Δ_1^0, Δ_2^0, σ_{Δ_1} and σ_{Δ_2} were extracted by the fit, they were related, by means of the AOM, to the distribution of the iron-heme displacement by introducing a Gaussian distribution for the iron-heme displacement around its average position. An example of the fit of the Δ_1 and Δ_2 distributions is shown in Fig. 2 from which it is clear that both the Δ_1 and Δ_2 distributions can be satisfactorily reproduced.

Results and discussion

An example of the reliability of the method employed to analyze the EPR spectra is reported in Fig. 3, in which a superposition of the experimental (continuous line) and the simulated (dashed line) spectrum of a pure Mb sample is shown. From a visual inspection the agreement between the two patterns appears very good; however, the

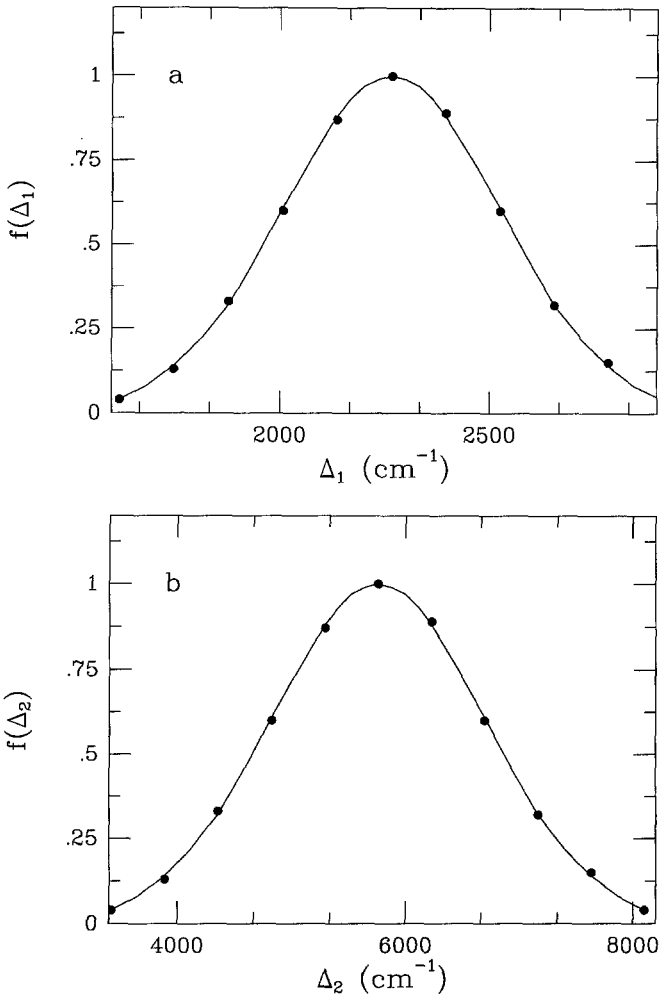

Fig. 2a,b. An example of the fits (*full circles*), derived from the AOM approach, of the crystal field parameter distributions (*continuous lines*) Δ_1 **a** and Δ_2 **b**, for a pure Mb sample

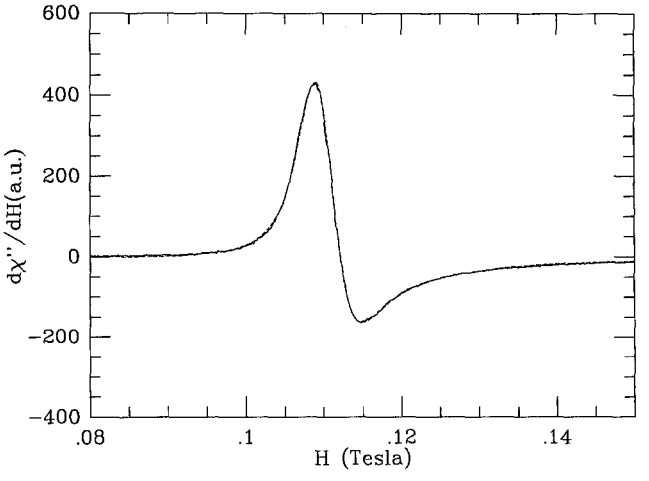

Fig. 3. Experimental (*continuous line*) and simulated (*dashed line*) X-band EPR spectrum, recorded at 77 K, restricted to the g=6 region of high spin ferric Mb sample in pure water ($\chi^2=0.71$). The spectrometer settings were: Microwave power level: 10 mW; Magnetic field sweep rate: 0.1 Tesla in 8 min; Time constant: 0.064 s; Modulation amplitude: 0.0005 Tesla; Modulation frequency: 100 kHz; Microwave frequency: 9.13 GHz

goodness of the fit has been confirmed by the χ^2-test. Similar results have been obtained for the fits of all the other Mb spectra. The values obtained for the Δ_1 and Δ_2 distributions appear to be consistent with the experimental values reported in the literature (Bizzarri and Cannistraro 1991, 1992a; Fiamingo et al. 1989).

Before analyzing the results in details, some considerations on the processes occurring in the Mb samples during the cooling process should be made. Upon decreasing the temperature, the bulk of the protein solution undergoes a liquid-solid phase transition that can be monitored by the appearance of a deep in the resonant cavity mode of the spectrometer where the cooling process is performed. Such a transition occurs at 240 K for pure Mb samples. When a glass-making solvent is used this temperature is lowered; i.e. in the presence of glycerol (1:1 by volume), the bulk solidification occurs at 220 K. We can imagine that the freezing of the bulk may reduce or even prevent CS transitions involving significant displacements or rearrangements of large parts of the protein molecule. On the other hand, since the freezing of the bulk occurs at a temperature higher than the protein glass-temperature T_g ($T_g = 220$ K for pure Mb samples and $T_g = 180$ K for samples with 75% of glycerol (Iben et al. 1989), transitions among CS may still be active even if the protein is embedded in a solid matrix. This fact shows the relevant role played by hydration water dynamics in the activation of the protein dynamics (Doster et al. 1986). Hydration water, that has been observed by NMR experiments to be not blocked above 200 K (Andrew et al. 1983), could contribute to the establishement of the protein structural heterogeneity, for a example according to a multiplicity of hydrogen bond networks on the protein surface (Doster et al. 1986).

A sort of strain around the active site, and in general in the overall protein structure, could be induced by the crystal growth at the phase transition of the bulk. Such an effect may be dependent on the solvent composition in the sense that the presence of some solvents, affecting the crystal dimensions, could result in a different strain in the protein structure. In this context, it can be remarked that the presence of possible artifacts in the ligand orientation of oxycobalt Mb have been observed to be induced by the freezing procedure (Hori et al. 1990). On the other hand, since the metal ion is not directly exposed to the external solvent, the possible freezing-induced effects on the iron should be considered as a main consequence of changes in the overall protein matrix rather than of a direct alteration produced on the heme group.

Figure 4 shows the Δ_1 and Δ_2 Gaussian distributions obtained by computer simulation, through Eq. (7), of the experimental spectra of Mb samples in solutions with different solvent compositions. The significant spreads displayed by these crystal field parameters (see the σ values reported inside Fig. 4) reflect the presence of a frozen ensemble of molecules, each one providing a slightly different ligand field to the FeIII ion; such a disorder arising from a modulation of the distances and/or the angles of the ligands with respect to the paramagnetic ion. From Fig. 4, it is also evident that the solvent composition affects the crystal field parameter distributions; Δ_2 appears

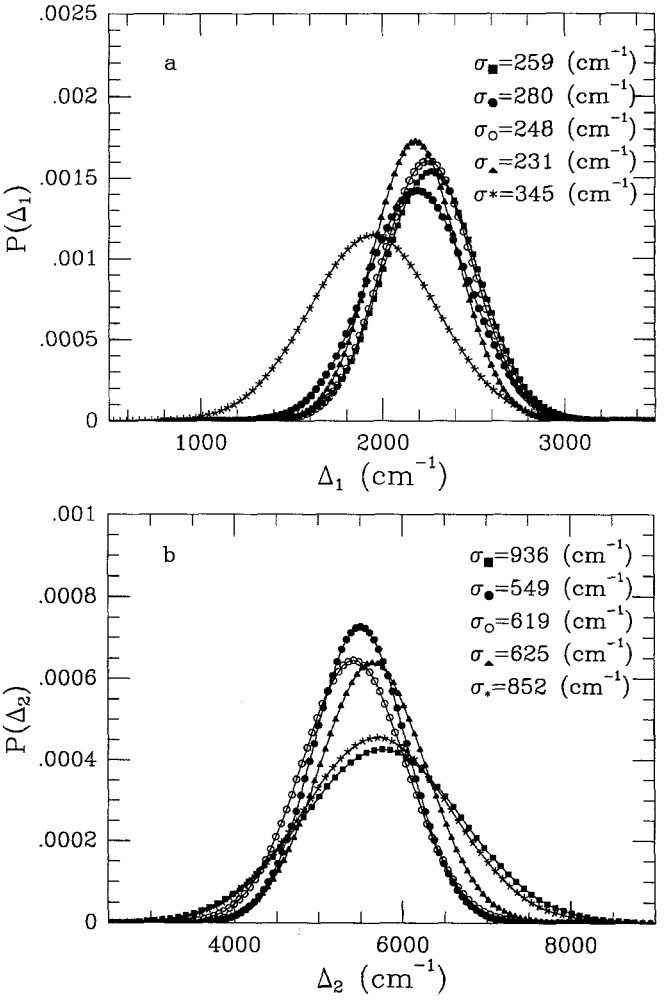

Fig. 4. Distributions of the crystal field parameters Δ_1 **a** and Δ_2 **b** for high spin ferric Mb samples under different conditions; (*full-square*) pure Mb; (*full-circle*) Mb in water-glycerol mixture (50% by volume); (*empty-circle*) Mb in water-ethylene glycol mixture (50% by volume); (*full-triangle*) Mb in water 1 M sucrose mixture (50% by volume); (star) Mb in water 1 M ammonium sulfate mixture (50% by volume). These distributions were obtained by simulation of the g=6 line, through Eq. (7), of the EPR spectra recorded at 77 K

to be the parameter most sensitive to changes in the protein milieu. In particular, addition of glycerol, ethylene glycol and sucrose produces a narrowing of the Δ_2 distribution, such an effect being particularly significant for glycerol. It should be remarked that, at variance with what happens with the addition of methanol and ethanol (Brill et al. 1986), the solvents used in the present investigations do not directly bind to the metal ion (Bizzarri and Cannistraro 1992a). Moreover, it has been reported that the biological activity of heme-proteins is not impaired in the presence of glycerol and ethylene glycol (Cordone et al. 1988). In addition, small shifts of the mean values of the Δ_2 crystal field parameter are caused by these solvents. Concerning Δ_1, the most significant change, in both the central values and in the variances, is registered in the presence of ammonium sulfate. A rationale for these results can be found when a distribution for the metal ion position, along the normal to the heme

plane, is considered. The gaussian distributions for the iron heme displacement, as extracted from the Δ_1 and Δ_2 distributions of Fig. 4, are shown in Fig. 5. It is notable that a significant spread for the iron-heme displacement characterizes all the analyzed Mb samples. The spread σ_a of pure Mb samples is about 0.06 Å. Such a value, smaller than those reported by other experimental techniques for FeII Mb samples (0.07–0.30 Å) (Frauenfelder et al. 1979; Srajer et al. 1988), can be justified by taking into account the higher oxidation state for the metal ion in our samples.

In general, the proximal histidine, which provides a nitrogen atom as a ligand to the metal ion, mediates the effects on the iron induced by changes in the protein matrix. Then, proximal histidine, assuming slightly different positions in the various frozen molecules, as can be shown from the X-ray diffraction studies (Parak et al. 1987; Frauenfelder et al. 1979), could induce a modulation in the iron position for the different CS. Therefore, the observed spread σ_a of the iron-heme displacement directly reflects the conformational substrate landscape of the protein molecules and can be assumed to be a suitable parameter to quantify the structural heterogeneity characterizing the protein frozen ensemble.

From Fig. 5, it is notable that glycerol, ethylene glycol and sucrose essentially induce a narrowing of the iron-heme displacement distribution while they do not modify in a significant way the average position of the iron. In contrast, addition of ammonium sulfate only slightly affects the width of the distribution, but produces a significant approach to the heme-plane of the iron average position. These substances, used at high concentrations, are expected to modify the water network and to induce some changes in the protein structure. Glycerol, an organic solvent widely employed in protein analysis and in optical spectroscopy to make samples transparent, is known to induce a sort of stabilization of the protein structure. In general, glycerol induces alterations in both the protein dynamics (by affecting the solvent viscosity) and the thermodynamic properties of the protein (Beece et al. 1980; Almagor et al. 1992). From the latter point of view, it is known that glycerol is preferentially excluded from the domain of the protein (first hydration shell) (Gekko and Timasheff 1981) with a subsequent raising of the chemical potential of the protein (Gekko and Timasheff 1981); such an effect being dependent on the glycerol concentration (Gekko and Timasheff 1981). As a consequence, to minimize the free energy, the system will tend to decrease the area of the solvent-protein contact through an enhancement of the protein self-association. On the other hand, such a packing of the protein stabilizes the protein itself by requiring more energy for its denaturation. In this context, it can be envisaged that large amplitude motions are unfavourable, that CS involving large residue displacements are no longer accessible and consequently, that the heterogeneity should be reduced. This seems to be the case especially when the results at different glycerol concentrations are analyzed. The trend of the iron-heme displacement distributions of Mb samples at three different glycerol concentrations (25%, 50% and 75% glycerol-water by volume) is shown in Fig. 6. It is evident that

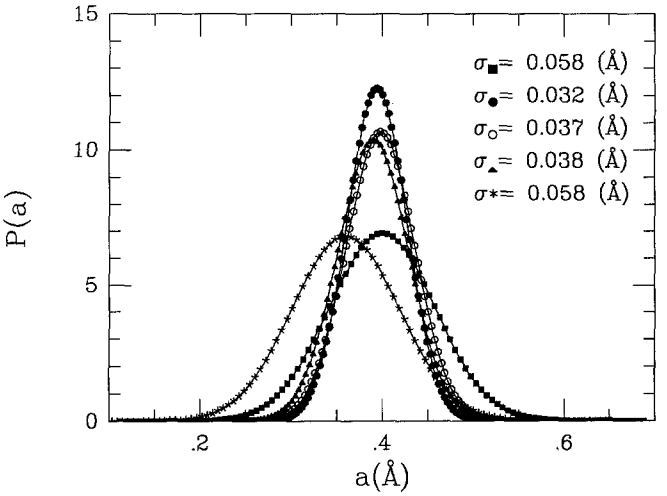

Fig. 5. Gaussian distributions of the iron-heme displacement for Mb samples under different conditions, as derived by the AOM approach (see text) from the Δ_1 and Δ_2 crystal field parameter distributions shown in Fig. 4; (*full-square*) pure Mb; (*full-circle*) Mb in water-glycerol mixture (50% by volume); (*empty-circle*) Mb in water-ethylene glycol mixture (50% by volume); (*full-triangle*) Mb in water 1 M sucrose mixture (50% by volume; (start) Mb in water 1 M ammonium sulfate mixture (50% by volume)

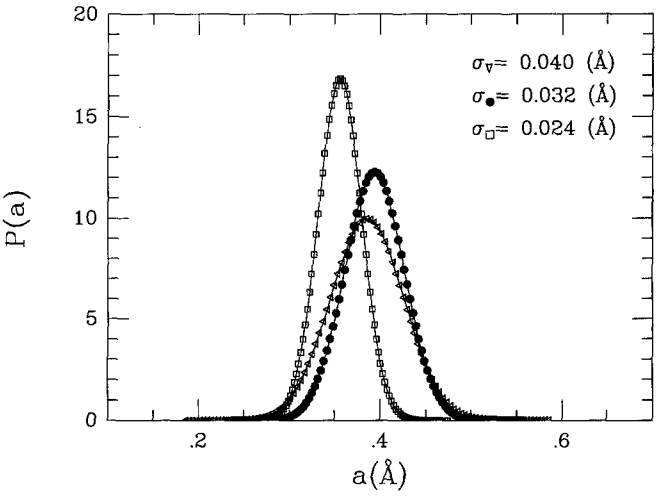

Fig. 6. Gaussian distributions of the iron-heme displacement for Mb samples in different conditions, as derived by the AOM approach (see text) from the Δ_1 and Δ_2 crystal field parameter distributions shown in Fig. 6; (*empty-triangle*) Mb in water-glycerol mixture (25% by volume); (*full-circle*) Mb in water-glycerol mixture (50% by volume); (*empty-square*) Mb in water-glycerol mixture (75% by volume)

an increase of the amount of glycerol present in the protein solution yields a narrowing of the iron-heme distribution. Moreover, at a glycerol concentration of 75% a significant approach of the average position of the metal ion to the heme-group can also be demonstrated. This evidence could indicate that the protein packing becomes much stronger at higher glycerol concentration. Nevertheless, some other mechanisms could be hypothesized in order to explain the reduction of σ_a by adding glycerol. For instance, the lowering of the dielectric constant ε of the solvent, as induced by glycerol, could result into a

stronger interaction among the charged aminoacid residues. Then, the protein dynamics might be affected so that the sampling of some CS would be prevented and, in turn, a decrease in the protein heterogeneity upon freezing could be registered. However, the effect on ε as induced by glycerol has been questioned (Lakshami and Nandi 1976). Another possible mechanism could be represented by the postulated decrease of the *H*-bond rupturing capacity of the medium as induced by the presence of glycerol (Gerlsma 1970). In the hypothesis that the presence of a multiplicity of water states is strictly coupled to the existence of the CS distribution (Doster et al. 1986), a slow down of the solvent dynamics, which is connected with a reduced heterogeneity in the water patches population, would be responsible for the reduced protein heterogeneity. Finally, as we have already mentioned, the presence of glycerol in the protein solution could induce a reduction in the crystal dimensions (Hagen 1981) when the freezing temperature is approached; such an effect, which should be dependent on the concentration, could be also invoked to explain the reduced heterogeneity of the protein system.

Eythylene glycol has chemico-physical properties in common with glycerol, so that the above mentioned mechanisms could be responsible for the effects displayed by this solvent on the protein molecule heterogeneity. The slightly smaller effects induced by ethylene glycol with respect to glycerol, is consistent with the results obtained by optical spectroscopy (Di Pace et al. 1992).

Sucrose, like glycerol, is preferentially excluded from the domain of the protein (Gekko and Timasheff 1981), and its presence in the protein solution also yields a stabilization of the protein itself (Gekko and Timasheff 1981). This effect is due to a molecular mechanism different from that which is operative in the presence of glycerol; in fact, sucrose essentially stabilizes the protein structure by means of an increase of the surface tension of water (Lee and Timasheff 1981). However, also in this case, the observed effects on the crystal field parameters, and on the iron-heme displacement, indicate a reduction of the protein heterogeneity. In general, it seems that every molecular mechanism leading to a stabilization of the protein structure can also lead to a reduction in the structural heterogeneity. Moreover, while glycerol molecules insert into the water structure, in a water-sucrose mixture, clusters of bulk water are separated by sucrose molecules (Gutman et al. 1992). Consequently, the freezing strain in solutions with sucrose is expected to be different from that occurring in a water-glycerol solution.

Finally, we consider the effects induced on Mb samples by the presence of ammonium sulfate, a salt widely employed in the purification and crystallization of the protein. It is known that an increase of the concentration of this salt results in a decrease of the Debye length of the counterionic cloud around the macromolecules (Stryer 1988). This effect, that is the basis of the salting out process, results in a sort of shrinking of the protein structure (Gabler 1978); in other words, the larger shielding of the electric charges of the amino-acid residues allows the protein to assume a more compact structure. The observed approach to the heme plane of the average position of the iron (see Fig. 6) suggests a modification in the environment of the heme-group possibly induced by some changes in the protein structure. On the other hand, it should be emphasized that no significant change in the spread of the iron position is observed, with respect to pure Mb solution; this means that the structural heterogeneity of the proteins is not significantly affected by the presence of this salt. This result is in agreement with the fact that since no significant variation in the viscosity is expected to be induced by ammonium sulfate, protein dynamics should not be affected in the presence of this salt. On the other hand, in the hypothesis that the solvent dynamics are responsible for the protein sample heterogeneity, such an effect might indicate that the multiplicity of the water states on the protein surface is not much modified by the addition of ammonium sulfate. In summary, the addition of ammonium sulfate causes a change of the overall protein structure and, at the same time, it does not induce any substantial alteration of the structural heterogeneity of the protein molecules, these results should be taken into account in the analysis of the results obtained for Mb crystals whose preparation requires ammonium sulfate.

Conclusions

EPR is a rewarding technique for investigating the structural heterogeneity of low temperature Mb solutions resulting from the presence of a frozen ensemble of molecules in different CS. The heterogeneity of the protein system can be quantified by the distribution of the iron-heme displacement, a geometrical parameter relevant for the biological function of the protein that can be extracted from the EPR spectra by the AOM. The significant modification of the protein structural heterogeneity, as induced by changes in the solvent composition, shows the important role played by the solvent in protein dynamics. These results should be taken into account in the analysis of data obtained by experimental techniques requiring the presence, in the Mb samples, of some substances. In particular, addition of glycerol, ethylene glycol (widely used in optical spectroscopy) and sucrose can result in a strong decrease of the structural heterogeneity of the protein system; moreover, the presence of ammonium sulfate (required to make Mb crystals) can induce a significant change in the iron-heme average position. Finally, it should be remarked that, since these results have been obtained at low temperature, possible freezing-induced effects cannot be ruled out; however, they are not peculiar to the particular technique employed but to the temperature at which measurements are performed. Then, they should be taken into account in the low temperature studies, independent of the particular technique applied.

References

Abragam A, Bleaney B (1970) Electron paramagnetic resonance of transition ions. Clarendon Press, Oxford

Almagor A, Yedgar S, Gavish B (1992) Viscous cosolvent effect on the ultrasonic absorption of bovine serum albumin. Biophys J 19:480–486

Andrew ER, Bryant DJ, Rizvi TZ (1983) The role of water in the dynamics of proton relaxation of solid proteins. Chem Phys Lett 95:463–466

Ansari A, Berendzen J, Bowne SF, Frauenfelder H, Iben IET, Sauke TB, Shyamsunder E, Young RD (1985) Protein states and proteinquakes. Proc Natl Acad Sci, USA 82:5000–5004

Ansari A, Berendzen J, Braunstein D, Cowen BR, Frauenfelder H, Hong MK, Iben IET, Johnson JB, Ormos P, Sauke TB, Scholl R, Schulte A, Steinback PJ, Vittitow J, Young RD (1987) Rebinding and relaxation in the myoglobin pocket. Biophys Chem 26:337–355

Bacci M (1979) Jahn-Teller effect in transition metal ions: a parametrization method based on the angular overlap method. Chem Phys 40:237–244

Bacci M (1980) Jahn-Teller effect in biomolecules. Biophys Chem 11:39–47

Bacci M, Cannistraro S (1990) Role of vibronic coupling and of conformational substate distribution in determining the feature of Copper-Protein EPR spectra. Appl Mag Res 1:369–378

Beece D, Eisenstein L, Frauenfelder H, Good D, Marden MC, Reinish L, Reynolds AH, Sorensen LB, Yue KT (1980) Solvent viscosity and protein dynamics. Biochemistry 19:5147–5157

Bizzarri AR (1992) Conformational substate distribution in high spin ferric myoglobin as studied by electron paramagnetic resonance. Ph. D. Dissertation (SISSA, International School for Advanced Studies, Trieste, Italy

Bizzarri AR, Cannistraro S (1991) An electron paramagnetic resonance study of conformational substate distribution in high spin heme-proteins. Appl Magn Res 2:627–645

Bizzari AR, Canistraro S (1992a) Solvent effects on myoglobin conformational substates as studied by electron paramagnetic resonance. Biophys Chem 42:79–85

Bizzarri AR, Cannistraro S (1992b) Conformational substate distribution in low spin ferric myoglobin as studied by electron paramagnetic resonance. Appl Magn Res 3:1033–1043

Bizzarri AR, Bacci M, Cannistraro S (1993) Distribution of the iron-heme displacement as resulting from myoglobin conformational substates: an AOM approach to the interpretation of the EPR spectra. Biophys Chem (in press 1993)

Brill AS, Fiamingo FG, Hampton DA (1986) EPR characterization of alcohol complexes of ferric myoglobin and hemoglobin. J Inorg Biochem 28:137–143

Burdett JK (1980) Molecular shapes-theoretical models of inorganic stereochemistry. Wiley, New York

Cannistraro S (1990) Distribution of conformational states as common source of g and A-strain in the ESR spectra of proteins and glasses. J Phys (France) 51:131–140

Cannistraro S, Giugliarelli G (1986) Field-swept and frequency-swept EPR copper spectra Computer Simulation in the presence of g and A-strain. Mol Phys 58:173–179

Cordone L, Cupane A, Leone M, Vitrano E, Bulone D (1988) Interaction between external medium and heme pocket in myoglobin probed by low temperature optical spectroscopy. J Mol Biol 199:213–218

Di Iorio EE, Hiltpold UR, Filipovic D, Winterhalter KH, Gratton E, Vitrano E, Cupane A, Leone M, Cordone L (1991) Protein dynamics. Comparative investigation on heme proteins with different physiological roles. Biophys J 59:742–754

Di Pace A, Cupane A, Leone M, Vitrano E, Cordone L (1992) Protein dynamics. Vibrational coupling, spectral broadening mechanisms, and anharmonicity effects in carbonmonoxy heme proteins studied by temperature dependence. Biophys J 63:475–484

Doster W, Bachleitner A, Dunau R, Hiebl M, Luscher E (1986) Thermal properties of water in myoglobin crystals and solutions at subzero temperatures. Biophys J 50:213–219

Doster W, Cusack S, Petry W (1989) Dynamic transition of myoglobin revealed by inelastic neutron scattering. Nature 337:754–756

Eisenberger P, Pershan PS (1967) Magnetic resonance studies of metmyoglobin and myoglobin azide. J Chem Phys 47:3327–3333

Elber R, Karplus M (1987) Multiple conformational states of proteins: a molecular dynamics analysis of myoglobin. Science 235:318–321

Fiamingo FG, Brill AS, Hampton DA, Thorkildsen R (1989) Energy distribution at the high-spin ferric sites in myoglobin crystals. Biophys J 55:67–77

Frauenfelder H, Petsko GA, Tsernoglou D (1979) Temperature-dependent X-ray diffraction as a probe of protein structural dynamics. Nature 280:558–563

Frauenfelder H, Parak F, Young RD (1988) Conformational substates in proteins. Ann Rev Biophys Biophys Chem 17:451–479

Gabler R (1978) Electrical interaction in moleculare biophysics. Academic Press, New York

Gavish B, Werber MM (1979) Viscosity-dependence structural fluctuations in enzime catalysis. Biochemistry 18:1269–1275

Gekko K, Timasheff SN (1981) Mechanism of protein stabilization by glycerol: preferential hydration in glycerol-water mixtures. Biochemistry 20:4667–4676

Gerlsma SY (1970) Effects of polyhydric and monohydric alcohols on the heat induced reversible denaturation of chemotripsinogen. Eur J Biochem 14:150–153

Giugliarelli G, Cannistraro S (1985) Simulation of EPR spectra of Cu^{2+} complexes with statistical distribution of the g-factor and hyperfine splitting. Chem Phys 98:115–122

Giugliarelli G, Tancini P, Cannistraro S (1989) IEEE-488 bus compatible computer interface for an EPR spectrometer. J Phys E (Sci Instrum) 22:702–708

Goldanski VI, Krupyanskii YF (1989) Protein and protein-bound water dynamics studied by Rayleigh scattering of Mössbauer radiation (RSMR). Q Rev Biophys 22:39–92

Gutman M, Nachliel E, Kiryati S (1992) Dynamic studies of proton diffusion in mesoscopic heterogeneous matrix I. concentrate solutions of sucrose. Biophys J 63:274–280

Hagen WR (1981) Dislocation strain broadening as a source of anisotropic linewidth and asymmetrical lineshape in the electron paramagnetic resonance spectrum of metallo-proteins and related systems. J Magn Res 44:447–469

Hagen WR, Hearshen DO, Sands RH, Dunham WR (1985) A statistical theory for powder EPR in distributed systems. J Magn Res 61:220–232

Hori H, Iketa-Saito M, Yoketani T (1990) Freezing induced change in ligand orientation in oxycobalt-myoglobin. Nature 288:501–502

Iben IET, Braunstein D, Doster W, Frauenfelder H, Hong MK, Johnson JB, Luck S, Ormos P, Schulte A, Steinbach PL, Xie AH, Young RD (1989) Glassy behaviour of a protein. Phys Rev Lett 62:1916–1919

Isomoto A, Watari H, Kotani M (1970) Dependence of EPR transition probability on magnetic field. J Phys Soc Jpn 29:1571–1577

Kirkpatrick S, Gelatt CD, Vecchi MP (1983) Optimization by simulated annealing. Science 220:671–680

Kotani M (1968) Paramagnetic properties and electronic structure of iron in heme proteins. Adv Quantum Chem 4:227–266

Lakshami TS, Nandi PK (1976) Effects of sugar solutions on the activity coefficients of aromatic amino acids and their N-acetyl ethyl esters. J Phys Chem 80:249–252

Lee JC, Timasheff SN (1981) The stabilization of proteins by sucrose. J Biol Chem 256:7193–7201

Marzola P, Cannistraro S (1992) Hydration and protein dynamics: an ESR and ST-ESR spin labelling study of human serum albumin. Appl Magn Res 3:1045–1060

Parak F, Knapp EW, Kucheida D (1982) Protein dynamics. Mössbauer spectroscopy on deoxymyoglobin crystals. J Mol Biol 161:177–194

Parak F, Hartmann H, Aumann KD, Reuscher H, Rennekamp G, Bartunik H, Steigemann W (1987) Low temperature X-ray investigation of structural distributions in myoglobin. Eur Biophys J 15:237–249

Peisach J, Blumberg WE, Ogawa S, Rachmilewitz EA, Oltzik R (1971) The effects of protein conformation on the heme symme-

try in high spin ferric heme proteins as studied by electron paramagnetic resonance. J Biol Chem 246:3342–3355
Schäffer CE (1967) The angular overlap method applied to chiral chromophores and the parentage interlation of absolute configurations. Proc R Soc A297:96–133
Scholes CP (1970) EPR studies on heme oriented in an organic crystalline environment. J Chem Phys 52:4890–4895
Singh GP, Parak F, Hunklinger S, Dransfeld K (1981) Role of the adsorbed water in the dynamics of metmyoglobin. Phys Rev Lett 47:685–688
Srajer V, Schomacke KT, Champion PM (1986) Spectral broadening in biomolecules. Phys Rev Lett 57:1267–1270
Srajer V, Reinisch L, Champion PM (1988) Protein fluctuations, distributed coupling, and the binding of ligands to heme proteins. J Am Chem Soc 110:6656–6670
Stryer L (1988) Biochemistry, 3rd edn. Freedman, New York
Takano T (1977) Structure of myoglobin refined at 2.0 Å resolution. I. Crystallographic refinement of metmyoglobin from sperm whale. J Mol Biol 110:537–568
Yang AS, Gaffney BJ (1987) Determination of relative spin concentration in some high-spin ferric proteins using E/D-distribution in electron paramagnetic resonance simulations. Biophys J 51:55–67